Physics Letters B 801 (2020) 135174

Contents lists available at ScienceDirect

Physics Letters B

www.elsevier.com/locate/physletb

Pseudospin and spin symmetries in single particle resonant states in Pb isotopes

Xin-Xing Shi (史新星)[a], Quan Liu (刘泉)[b,*], Jian-You Guo (郭建友)[b,*], Zhong-Zhou Ren (任中洲)[a,c]

[a] School of Physics, Nanjing University, Nanjing 210093, PR China
[b] School of Physics and Materials Science, Anhui University, Hefei 230601, PR China
[c] School of Physics Science and Engineering, Tongji University, Shanghai 200092, PR China

ARTICLE INFO

Article history:
Received 14 October 2019
Received in revised form 18 December 2019
Accepted 18 December 2019
Available online 27 December 2019
Editor: W. Haxton

Keywords:
Pseudospin symmetry
Spin symmetry
Resonant states
Relativistic mean field

ABSTRACT

Based on the newly developed RMF-CMR theory by combining relativistic mean field (RMF) with complex momentum representation (CMR), we have explored the single particle resonant states, and their pseudospin and spin symmetries for Pb isotopes. The available energies and widths decrease monotonously with the increasing mass number in accompany with clear shell structure including the appearance of magic number $N = 184$. The extracted pseudospin and spin splittings become smaller for the neutron-richer nuclei. The extent of the splittings depends on the quantum numbers and position of the states lying in mean field. Good pseudospin and spin symmetries are expected in the neutron-rich nuclei and the states with lower orbital momentum and lying near the continuum threshold. Especially, it is found that both lower (upper) components of the every pseudospin (spin) doublet look similar for not only bound states but also resonant states, which confirms the presence of the pseudospin (spin) symmetry although the corresponding energy splitting is slightly large.

1. Introduction

It is well known that the spin and pseudospin symmetries play important role at nuclear structure [1–4]. The breaking of spin symmetry between the doublets marked by the quantum numbers $(n, l, j = l \pm 1/2)$ has clarified the existence of magic numbers [5,6]. The quasi-degenerate states with the quantum numbers $(n, l, j = l + 1/2)$ and $(n - 1, l + 2, j = l + 3/2)$ regarded as pseudospin doublets $(\tilde{n} = n, \tilde{l} = l + 1, \tilde{j} = \tilde{l} \pm 1/2)$ [7–9] have explained numerous nuclear phenomena, such as identical bands [10,11], pseudospin partner bands [12,13], shape coexistence in the ^{78}Ni region [14], and so on.

Since the success of pseudospin symmetry (PSS) in explaining various nuclear phenomena, much effort is devoted to explore the origin of this symmetry. Based on the relativistic mean field theory (RMF), Ginocchio has made a substantial progress [15], and pointed out that this symmetry is a relativistic symmetry, which arises from an approximate equality in magnitude of the scalar S and vector V potentials, but opposite sign. When $V + S = 0$, this symmetry is exact. Meng *et al.* extended the condition to a general case $V + S =$ const in the pseudospin symmetry limit [16]. To clarify the relativistic origin of PSS, the SU(2) algebra was established for the Dirac Hamiltonian [17], just like that of spin symmetry [18]. In the (pseudo)spin symmetry limit, the Dirac Hamiltonian with special potentials was shown to possess U(3) symmetry [19] and chiral symmetry [20,21]. The supersymmetric description of the Dirac Hamiltonian was presented in Refs. [22,23]. The nonperturbation nature of PSS was recognized in Refs. [24,25].

Despite these researches, the origin of pseudospin symmetry has not been fully understood. In Refs. [26,27], we have applied the similarity renormalization group (SRG) to transform the Dirac Hamiltonian into a diagonal form. Based on the diagonal Dirac Hamiltonian, the quality of pseudospin approximation is shown to be related to the competition between the spin-orbit coupling and dynamical effect [28–30]. In combination with supersymmetric quantum mechanics and perturbation theory, this Hamiltonian has been used to investigate the nonperturbation nature of PSS [31, 32], and the isospin asymmetry of PSS [33]. More researches on the PSS can be found in these reviews [1,2] and references therein. Recent progresses include spin and pseudospin symmetries in the single-Λ spectrum [34], temperature effects on nuclear pseudospin symmetry in the Dirac-Hartree-Bogoliubov formalism [35], spin

* Corresponding authors.
E-mail addresses: quanliu@ahu.edu.cn (Q. Liu), jianyou@ahu.edu.cn (J.-Y. Guo).

https://doi.org/10.1016/j.physletb.2019.135174

symmetry in the Dirac sea derived from the bare nucleon-nucleon interaction [4]. An extension and optimization of SRG for expansion of Dirac Hamiltonian is discussed in Ref. [36].

These investigations on the pseudospin symmetry focus mainly on the single particle spectrum of bound states in stable nuclei. In recent years, the nuclei far from the stability line have received additional attention for appearance of many exotic phenomena [37]. One of the most interesting phenomena is the disappearance of traditional magic numbers and occurrence of new magic numbers, where the spin and pseudospin symmetries play important role [38,39]. Considering that the change of magic numbers occurs in the weakly bound nuclei, and is very related to the level structure of resonant states [40], it is necessary to explore the resonant states. At present, several methods have been developed for resonant states, such as R-matrix method [41], S-matrix theory [42], Jost function approach [43,44], the analytical continuation of the coupling constant method [45–48], Green's function method [49, 50], the complex scaling method [51–53], and the complex-scaled Green's function method [54–58]. In comparison with these methods, the complex momentum representation (CMR) holds many advantages including that the bound states and resonant states can be treated on an equal footing, and narrow resonances and broad resonances can be obtained simultaneously. More advantages can be found in Refs. [59,60].

Due to the advantages of CMR, we have combined the CMR with RMF [59], and established the RMF-CMR theory. The RMF-CMR theory is able to describe self-consistently nuclear bound states and resonant states in the relativistic framework. In this paper, we apply the RMF-CMR theory to explore the single particle resonant states and check the corresponding pseudospin symmetry in comparison with the bound states for Pb isotopes. Considering the spin symmetry, which play important at nuclear shell structure, holds the same origin as the pseudospin symmetry [28,59], we have also checked the spin symmetry for the available bound and resonant states in Pb isotopes. In Sec. 2, we sketch the theoretical formalism. The numerical details and results are presented in Sec. 3. A summary is given in Sec. 4.

2. Formalism

In order to investigate the (pseudo)spin symmetry in resonant states, we introduce the theoretical formalism of the RMF-CMR theory. In the RMF theory [61–63], nucleons are described as Dirac particles interacting via the exchange of various mesons (σ, ω^μ, and ρ^μ), and photons, the Lagrangian density of the model can be written as

$$\begin{aligned}\mathcal{L} = &\bar{\psi}\left(i\gamma_\mu\partial^\mu - M\right)\psi + \frac{1}{2}\partial_\mu\sigma\partial^\mu\sigma - U(\sigma) - \frac{1}{4}\Omega_{\mu\nu}\Omega^{\mu\nu} \\ &+\frac{1}{2}m_\omega^2\omega_\mu\omega^\mu - \frac{1}{4}\vec{R}_{\mu\nu}\vec{R}^{\mu\nu} + \frac{1}{2}m_\rho^2\vec{\rho}_\mu\vec{\rho}^\mu - \frac{1}{4}F_{\mu\nu}F^{\mu\nu} \\ &-\bar{\psi}\left(g_\sigma\sigma + g_\omega\gamma_\mu\omega^\mu + g_\rho\gamma_\mu\vec{\tau}\vec{\rho}^\mu + e\gamma_\mu A^\mu\right)\psi, \end{aligned} \tag{1}$$

where M is nucleon mass and ψ is Dirac spinor. m_σ, m_ω, and m_ρ are the masses of the respective mesons. The coupling constants are g_σ, g_ω, and g_ρ, respectively. A^μ is the photon field. The non-linear couplings of the scalar meson (σ) read $U(\sigma) = \frac{1}{2}m_\sigma^2\sigma^2 + \frac{1}{3}g_2\sigma^3 + \frac{1}{4}g_3\sigma^4$. Based on the Lagrange density, the Dirac equation is written as

$$\left[\vec{\alpha}\cdot\vec{p} + \beta(m+S) + V\right]\psi_i = \varepsilon_i\psi_i, \tag{2}$$

for nucleons with the scalar and vector potentials

$$\begin{cases} S(\vec{r}) = g_\sigma\sigma(\vec{r}), \\ V(\vec{r}) = g_\omega\omega^0(\vec{r}) + g_\rho\tau_3\rho^0(\vec{r}) + eA^0(\vec{r}). \end{cases} \tag{3}$$

In order to obtain the solutions of bound states and resonant states, the equation (2) is transformed into momentum representation

$$\int d\vec{k}'\left\langle\vec{k}\right|H\left|\vec{k}'\right\rangle\psi\left(\vec{k}'\right) = \varepsilon\psi\left(\vec{k}\right), \tag{4}$$

where $H = \vec{\alpha}\cdot\vec{p} + \beta\left(m + S\left(\vec{r}\right)\right) + V\left(\vec{r}\right)$. For spherical nuclei, the momentum wavefunction $\psi\left(\vec{k}\right)$ can be assumed as

$$\psi\left(\vec{k}\right) = \begin{pmatrix} f(k)\phi_{ljm_j}(\Omega_k) \\ g(k)\phi_{\tilde{l}jm_j}(\Omega_k) \end{pmatrix}, \tag{5}$$

so the Dirac equation for a spherical system becomes

$$\begin{cases} Mf(k) - kg(k) + \int k'^2dk'V_+\left(k,k'\right)f(k') = \varepsilon f(k), \\ -kf(k) - Mg(k) + \int k'^2dk'V_-\left(k,k'\right)g(k') = \varepsilon g(k), \end{cases} \tag{6}$$

with

$$V_+\left(k,k'\right) = \frac{2}{\pi}\int r^2dr\left[V(r) + S(r)\right]j_l\left(k'r\right)j_l(kr), \tag{7}$$

$$V_-\left(k,k'\right) = \frac{2}{\pi}\int r^2dr\left[V(r) - S(r)\right]j_{\tilde{l}}\left(k'r\right)j_{\tilde{l}}(kr). \tag{8}$$

By solving the above equations in complex momentum space, the bound and resonant states are obtained simultaneously. The details can be seen in Ref. [59]. The upper and lower components of wavefunctions in coordinate representation can be calculated by the following formulas

$$\begin{cases} f(r) = i^l\sqrt{\frac{2}{\pi}}\int k^2dkj_l(kr)f(k), \\ g(r) = i^{\tilde{l}}\sqrt{\frac{2}{\pi}}\int k^2dkj_{\tilde{l}}(kr)g(k). \end{cases} \tag{9}$$

3. Result and discussion

With the formalism presented above, we explore the single particle resonant states and their pseudospin and spin symmetries for Pb isotopes. The calculated energies for resonant states are displayed in Fig. 1 with several bound levels for comparison. With the increasing of mass number from $A = 190$ to 220, the resonance energies decrease monotonically. This trend is in accordance with that of bound states near the continuum threshold, but differs from that of the deeply bound states. Similar to the bound levels, there appear several large energy gaps in the resonant levels including the traditional magic number $N = 184$. Several new energy gaps in $N = 224$ and $N = 250$ expect to be confirmed in experiment. With the development towards the neutron rich nuclei, there appear the level crossings near the zero energy surface, which is helpful to understand the evolution from the bound states to the resonant states.

The available widths of resonant states are displayed in Fig. 2. With the increasing of mass number, the widths decrease monotonically. Widths for broader resonant states, such as these states $2i_{11/2}$, $2i_{13/2}$, $3f_{5/2}$, and $3f_{7/2}$, decrease rapidly than those for narrower resonant states. Similar to the energies, there appear several gaps among the widths, as seen the gap between the levels $2i_{11/2}$ and $3f_{5/2}$, and that between the levels $3f_{7/2}$ and $1k_{15/2}$. This knowledge on widths is useful to understand the exotic phenomena in nuclei because it reflects the stability of resonant states.

Based on these available energies and widths, we explore the pseudospin and spin symmetries in resonant states. In Refs. [64, 50], the pseudospin symmetry in resonant states has been investigated by solving the Dirac equation with Woods-Saxon type potential by ACCC approach [64] and Green's function method [50]. The

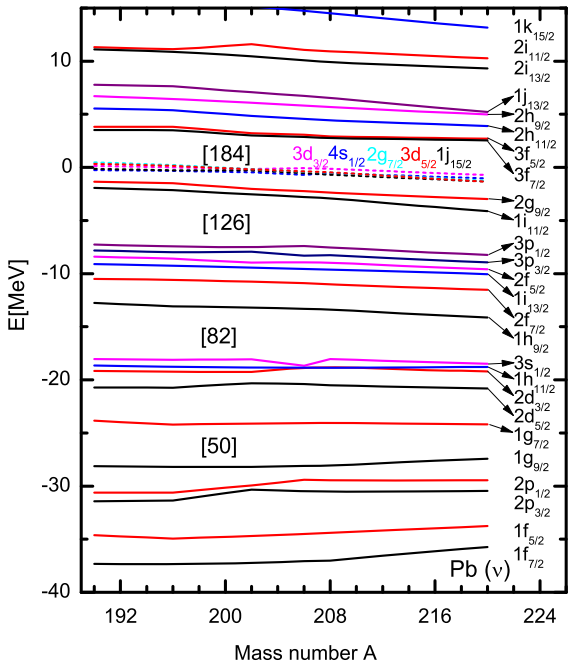

Fig. 1. The neutron single particle energies as a function of mass number in Pb isotopes. The labels of single particle states are marked in the right side and that of the five states near the continuum threshold are marked above of these levels with the corresponding colors.

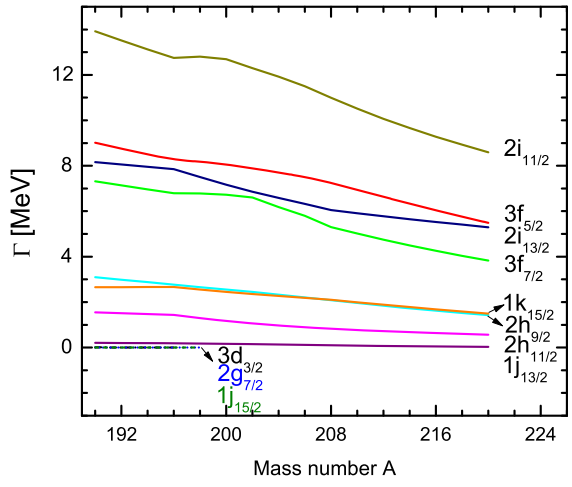

Fig. 2. The same as Fig. 1, but for the resonance widths.

parameters of Woods-Saxon potential are determined by fitting the mean field from the RMF calculations for ^{208}Pb. Considering that the RMF theory is appropriate to not only stable nuclei but also exotic nuclei, and CMR method is effective for not only narrow resonances but also broad resonances, the RMF-CMR theory should be more reliable for the exploration of resonant states and relativistic symmetries in real nuclei.

The energy and width splittings between the doublets near the continuum threshold and their evolutions to mass number are presented in Fig. 3 for the eight pseudospin doublets $3\tilde{p}$, $2\tilde{d}$, $2\tilde{f}$, $2\tilde{g}$, $1\tilde{g}$, $1\tilde{h}$, $1\tilde{i}$, and $1\tilde{j}$. Over the Pb isotopes considered here, $2\tilde{g}$, $1\tilde{i}$, and $1\tilde{j}$ are resonant pseudospin doublets, and $2\tilde{d}$, $1\tilde{g}$, $1\tilde{h}$ are bound pseudospin doublets, while $3\tilde{p}$, $2\tilde{f}$ evolve from resonant states to bound states with the increasing of mass number.

For every resonant pseudospin doublet except for these states very close to the zero energy surface, the energy of the pseudospin

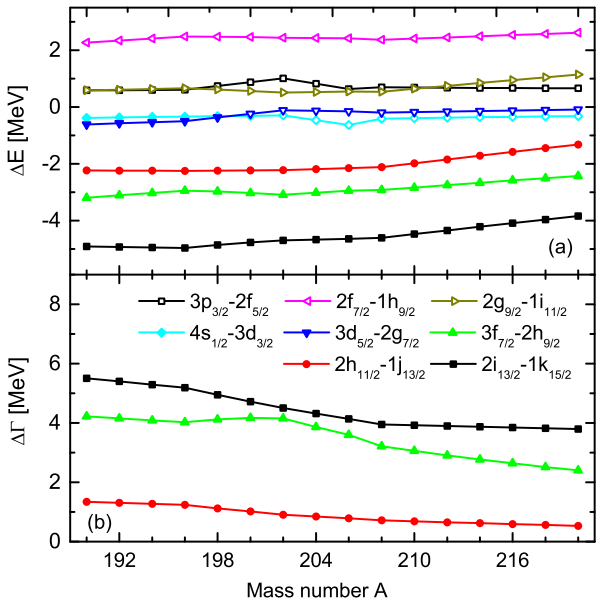

Fig. 3. The energy and width splittings of pseudospin doublets in Pb isotopes. The filled and opened labels respectively denote the resonant and bound states.

unaligned state is smaller than that of the pseudospin aligned state, i.e., $E_{n,l,j=l+1/2} < E_{n-1,l+2,j=l+3/2}$, which is opposite to that of the bound states. With the increasing of mass number, the pseudospin energy splittings for resonant states become small, while those for bound states become large. A good pseudospin symmetry for resonant states is expected in the neutron-rich nuclei. For the pseudospin doublets very close to the zero energy surface, such as the doublets $(4s_{1/2}, 3d_{3/2})$ and $(3d_{5/2}, 2g_{7/2})$, the pseudospin energy splitting is very small and insensitive to isospin. Namely, the pseudospin symmetry is better for these doublets closer to the zero energy surface.

For the resonant pseudospin doublets with the same radial quantum number n, the pseudospin energy splittings are smaller for the doublets with lower angular momentum. For example, the energy splitting between the pseudospin doublet $(2h_{11/2}, 1j_{13/2})$ is a half smaller than that of the doublet $(2i_{13/2}, 1k_{15/2})$. The result is opposite to that of the bound pseudospin doublets, as seen that the energy splitting between the pseudospin doublet $(2f_{7/2}, 1h_{9/2})$ is 2 MeV larger than that of the doublet $(2g_{9/2}, 1i_{11/2})$. For the pseudospin doublets with the same orbital angular momentum $\tilde{l}$, the pseudospin energy splitting is different for the doublets with different radial quantum number n. For example, the pseudospin energy splitting between the bound doublet $(2f_{7/2}, 1h_{9/2})$ is greater than zero, while that between the resonant doublet $(3f_{7/2}, 2h_{9/2})$ is smaller than zero.

Different from the energy splittings, the pseudospin width splittings decrease monotonously with the increasing mass number. For every pseudospin doublet, the width of pseudospin unaligned state is larger than that of pseudospin aligned states, i.e., $\Gamma_{n,l,j=l+1/2} > \Gamma_{n-1,l+2,j=l+3/2}$. It indicates that the pseudospin aligned state is more stable than the corresponding pseudospin unaligned state. For the pseudospin doublets with the same radial quantum number n, the width splittings between the pseudospin doublets with higher orbital angular quantum are larger than that with lower orbital angular quantum, which is in accordance with the pseudospin energy splittings. These indicate the quality of pseudospin symmetry is correlated with the quantum numbers of single particle states, isospin, and position of the states lying in the mean field. A good pseudospin symmetry is inclined to these states with

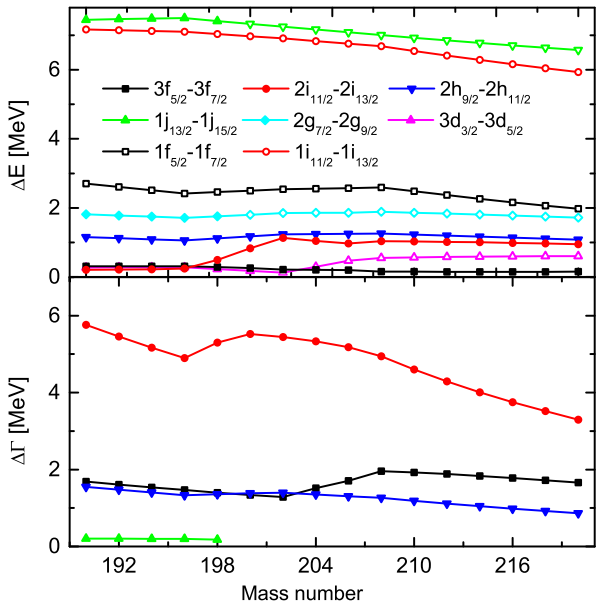

Fig. 4. The same as Fig. 3, but for the spin doublets. The filled and opened labels respectively denote the resonant and bound states.

lower orbital momentum and lying near the continuum threshold. The conclusion is in agreement with that obtained in Refs. [64,50].

For comparison, we have also investigated the spin symmetry in resonant states. The energy and width splittings between the spin doublets are shown respectively in the upper and lower panels in Fig. 4. For every spin doublet, the energy of the spin unaligned state with the quantum numbers $(n, l, j = l - 1/2)$ are larger than that of the spin aligned state with the quantum numbers $(n, l, j = l + 1/2)$. With the increasing of mass number, the spin energy splitting decreases with a few exceptions. For the resonant spin doublets with the same radial quantum number, such as these doublets $(2h_{9/2}, 2h_{11/2})$ and $(2i_{11/2}, 2i_{13/2})$, the spin energy splittings decrease with the increasing orbital angular momentum, which is opposite to that of the bound states as seen in these doublets $(1f_{5/2}, 1f_{7/2})$ and $(1i_{11/2}, 1i_{13/2})$. Moreover, the energy splittings between the resonant spin doublets are relatively small in comparison with that of the bound states with the $(3d_{3/2}, 3d_{5/2})$ exception, which is very close to the zero energy surface.

Similar to the energy, the width of the spin unaligned state with the quantum numbers $(n, l, j = l - 1/2)$ is larger than that of the spin aligned state with the quantum numbers $(n, l, j = l + 1/2)$, which is similar to that of pseudospin doublet. The width splittings decrease with the increasing of mass number with a bit exception like the doublet $(3f_{5/2}, 3f_{7/2})$ in ^{204}Pb. For the resonant spin doublets with the same radial quantum number, for examples the doublets $(2h_{9/2}, 2h_{11/2})$ and $(2i_{11/2}, 2i_{13/2})$, the width splittings increases with the increasing orbital angular momentum. These indicate the quality of spin symmetry is also related to the quantum numbers of single-particle states, isospin, and position of the state lying in mean field. A good spin symmetry is expected in these doublets with lower orbital angular momentum and lying near the zero energy surface.

The previous result show, except for these states very close to the zero energy surface, that the energy (width) splittings between the pseudospin doublets are considerably large for all the available resonant states. Similar case also appears in the spin doublets. To find out whether there are the pseudospin and spin symmetries in these resonant states, it is necessary to compare the wave functions of these doublets.

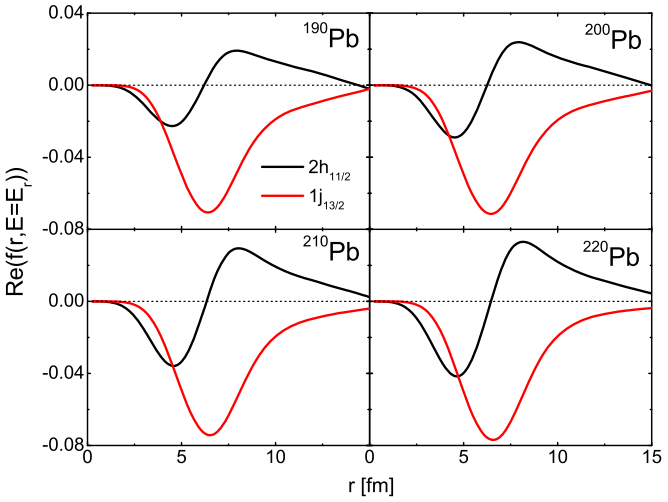

Fig. 5. Real parts of the upper components of Dirac spinors for the resonant pseudospin doublet $(2h_{11/2}, 1j_{13/2})$ in ^{190}Pb, ^{200}Pb, ^{210}Pb, and ^{220}Pb.

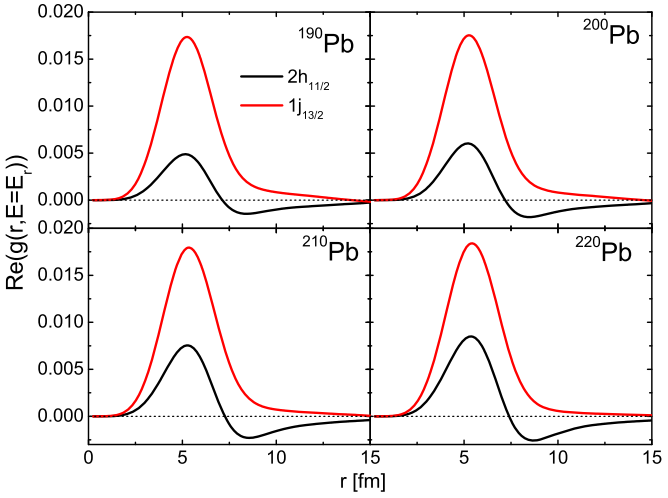

Fig. 6. The same as Fig. 5, but for the lower component of Dirac spinors.

Real parts of the upper components of Dirac spinors for the pseudospin doublet $(2h_{11/2}, 1j_{13/2})$ are plotted in Fig. 5. The upper component of the state $2h_{11/2}$ is different from that of the state $(1j_{13/2})$ for all the Pb isotopes considered here. Nevertheless, the number of radial nodes satisfies the relation $n(\kappa < 0) = n(\kappa > 0) + 1$ within the region of $r < 15$ fm, which means the existence of pseudospin symmetry, as indicated in Refs. [3,65] for the bound pseudospin doublets.

As the pseudo-orbital angular momentum is this orbital angular momentum of the lower component of Dirac spinors [15], the two lower components of pseudospin doublet are identical in the exact pseudospin symmetry limit. Hence, to judge the existence of pseudospin symmetry, it is necessary to compare the similarity of the lower components of pseudospin doublet. For this reason, we have plotted the lower components of Dirac spinors for the doublet $(2h_{11/2}, 1j_{13/2})$ in Fig. 6, where the negligible imaginary parts are omitted. In addition to the difference in magnitude, the two lower components look very similar, which confirms the existence of pseudospin symmetry in the resonant doublets.

For comparison, we have also plotted the wave function of the pseudospin doublet for bound states. The upper components of Dirac spinors for the doublet $(2g_{9/2}, 1i_{11/2})$ are shown in Fig. 7. Similar to the resonant pseudospin doublet $(2h_{11/2}, 1j_{13/2})$, there

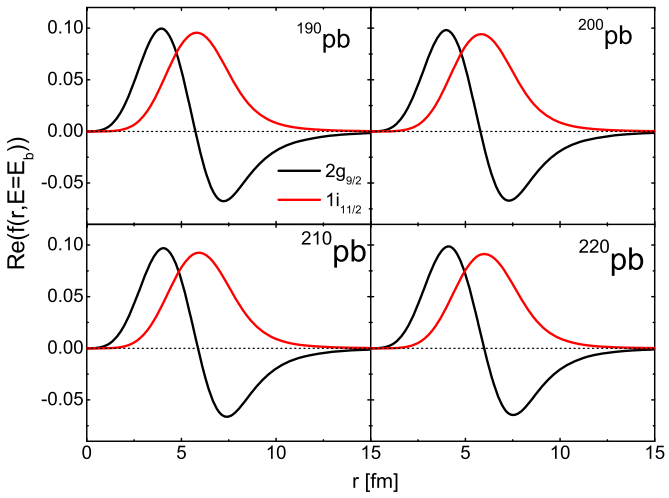

Fig. 7. The upper components of Dirac spinors $f(r)$ for the bound pseudospin doublet $(2g_{9/2},\ 1i_{11/2})$ in ^{190}Pb, ^{200}Pb, ^{210}Pb, and ^{220}Pb.

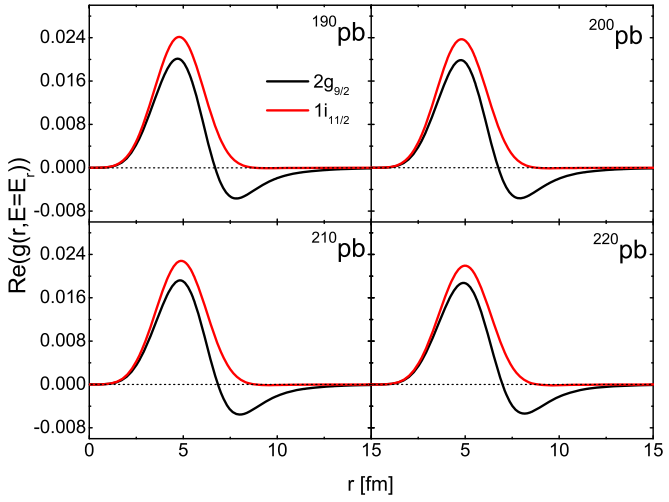

Fig. 8. The same as Fig. 7, but for the lower component of Dirac spinors $g(r)$.

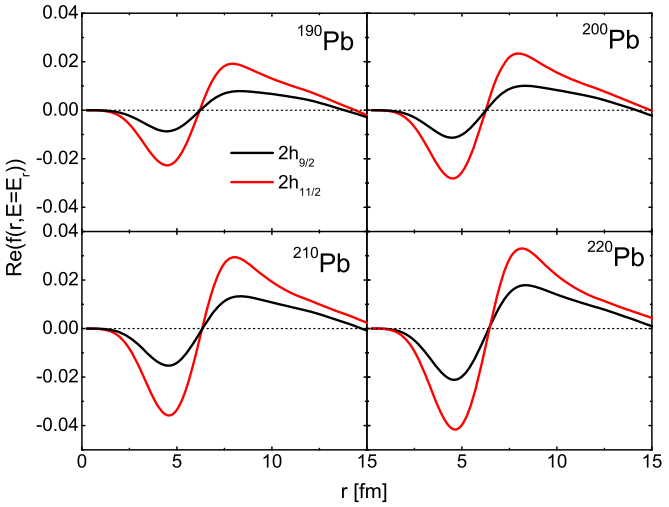

Fig. 9. Real part of the upper components of Dirac spinors $f(r)$ for the resonant spin doublet $(2h_{9/2},\ 2h_{11/2})$ in ^{190}Pb, ^{200}Pb, ^{210}Pb, and ^{220}Pb.

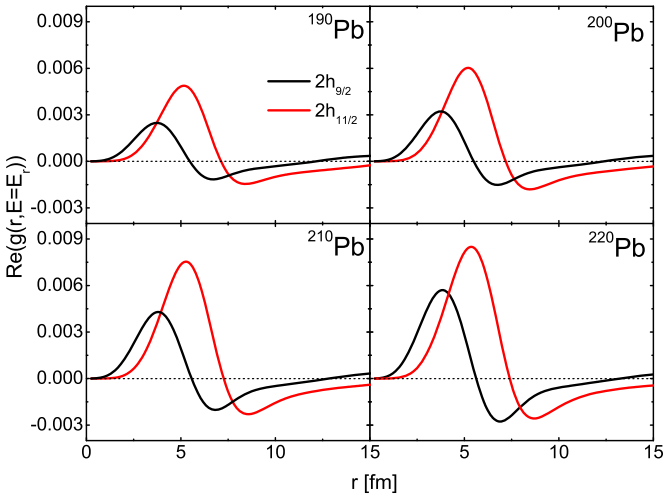

Fig. 10. The same as Fig. 9, but for the lower component of Dirac spinor $g(r)$.

are significant difference in the two upper components of Dirac spinors. But the radial-node number satisfies the same relation $n(\kappa<0)=n(\kappa>0)+1$ within the region of $r<15$ fm, which means the existence of pseudospin symmetry, as indicated in Refs. [3,65]. Because the $(2g_{9/2},\ 1i_{11/2})$ are bound states, the spatial convergence of wave functions is very well, the relation of radial node number is better satisfied. These mean that the upper components of wave functions meet the condition of pseudospin symmetry in resonant states as well as bound states.

Considering that the similarity of the lower components of Dirac spinors is a direct criterion of pseudospin symmetry, we compare the lower components of Dirac spinors for the bound pseudospin doublets $(2g_{9/2},\ 1i_{11/2})$, which are plotted in Fig. 8. Compared with the resonant doublets $(2h_{11/2},\ 1j_{13/2})$, the lower components of Dirac spinors $(2g_{9/2},\ 1i_{11/2})$ are more similar, which indicates that the pseudospin symmetry in the bound doublet $(2g_{9/2},\ 1i_{11/2})$ is better than that in the resonant doublet $(2h_{11/2},\ 1j_{13/2})$. The conclusion is supported by the single particle levels, the energy splitting between the doublet $(2g_{9/2},\ 1i_{11/2})$ is almost a half of that of the doublet $(2h_{11/2},\ 1j_{13/2})$, which can be seen in Fig. 3 over the Pb isotopes considered here. These indicate there are good pseudospin symmetry in resonant states and bound states although their energy splittings are quite large. Compared with resonant states, the wave functions of bound states satisfy better the pseudospin symmetry.

Similar to the pseudospin symmetry, the energy (width) splittings between the spin doublets are rather large for all the available resonant states except for those very close to the zero energy surface. To clarify whether there is a spin symmetry in these resonant states, it is necessary to compare the wave functions of these spin doublets.

As the upper components of Dirac spinors for every spin doublet are identical in the spin symmetry limit, to check the similarity of the upper components is helpful to understand the quality of spin symmetry. The upper components of the Dirac spinors for the doublet $(2h_{9/2},\ 2h_{11/2})$ are shown in Fig. 9. Although there are large difference in magnitude, the two upper components look similar. Namely, the spin symmetry is reserved for all the Pb isotopes considered here.

Compared with the upper components, the difference between the two lower components is considerably significant, as seen in Fig. 10 for the doublet $(2h_{9/2},\ 2h_{11/2})$. But, their radial node number meets the relation $n(\kappa>0)=n(\kappa<0)+1$, which means the existence of spin symmetry.

For comparison, we have also plotted the wave functions for the bound spin doublet. The upper components of the spin dou-

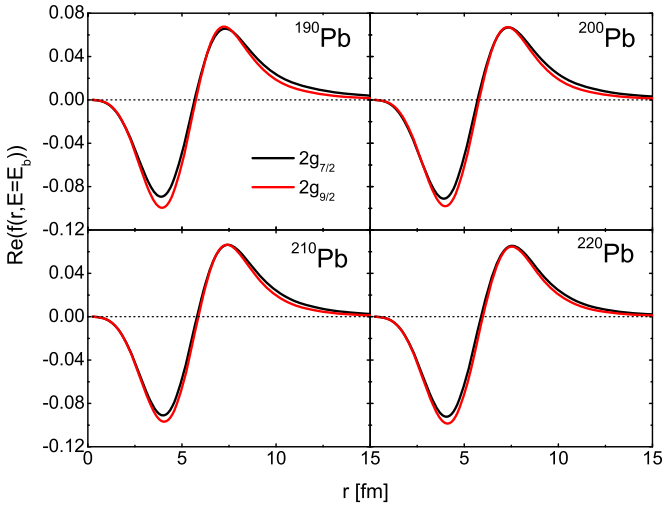

Fig. 11. The upper components of Dirac spinors $f(r)$ for the bound spin doublet $(2g_{7/2}, 2g_{9/2})$ in ^{190}Pb, ^{200}Pb, ^{210}Pb, and ^{220}Pb.

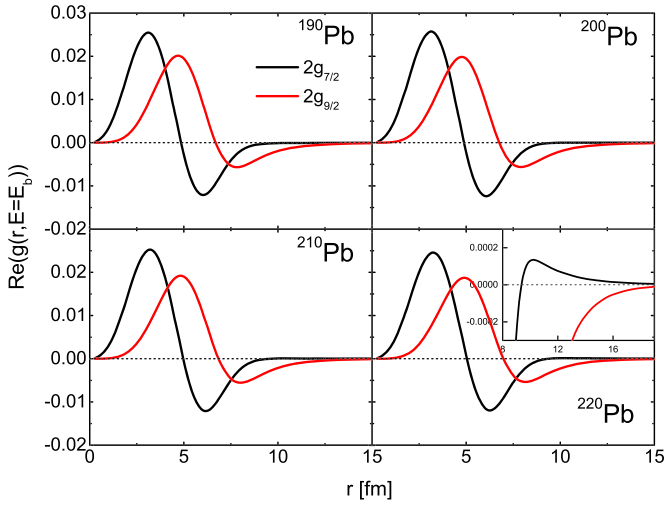

Fig. 12. The same as Fig. 11, but for the lower components of Dirac spinor $g(r)$. To show clearly the relation of radial node number, an inset is added in the fourth subfigure.

blet $(2g_{7/2}, 2g_{9/2})$ are shown in Fig. 11. From the figure, it can be seen that the two upper components are very similar. From the point of view of wave functions, the two states hold good spin symmetry although their energy splitting is considerately large. In comparison with the resonant spin doublet $(2h_{9/2}, 2h_{11/2})$, the spin symmetry in the bound spin doublet $(2g_{7/2}, 2g_{9/2})$ is better.

Similar to the resonant states, the lower components of bound states between the spin doublets are also different, as seen in Fig. 12 for the spin doublet $(2g_{7/2}, 2g_{9/2})$. The detailed observation shows their radial node number satisfies the same relation as that of the resonant spin doublet (to see the inset in the forth subfigure in Fig. 12), which supports the spin symmetry in the lower components of Dirac spinors for bound states.

In conclusion, although there are large pseudospin and spin energy splittings, the wave functions of these doublets satisfy well the conditions of the corresponding pseudospin and spin symmetries regardless of bound or resonant states, which confirms the inference in Ref. [50].

4. Summary

The level structure of single particle resonant states is one of the important characteristics reflecting nuclear shell structure especially for exotic nuclei. We apply the RMF-CMR theory to explore the single particle resonant states and their pseudospin and spin symmetries for Pb isotopes. The available energies and widths of resonant states decrease monotonically with the increasing mass number in accompanying with clear shell structure including the appearance of the traditional magic number $N = 184$. The extracted pseudospin and spin splittings are correlated with the quantum numbers of single particle states and position of the states lying in mean field. For the pseudospin doublets with the same radial quantum number, the energy splittings decrease with the increasing orbital angular momentum. The same case also appears in the spin doublets. However for the width, the evolution of spin splitting to the orbital angular momentum is opposite to that of pseudospin splitting. The pseudospin and spin symmetries are also related to the isospin, the energy and width splittings between the pseudospin (spin) doublets decrease with the increasing neutron number in Pb isotopes. Compared with the bound states, the pseudospin (spin) energy splittings of resonant states are relatively large (small). Good pseudospin and spin symmetries appear in these states very close to the zero energy surface.

Although the pseudospin and spin energy splittings are a bit large for these states far slightly from the zero energy surface, the wave functions satisfy the corresponding symmetries. For every pseudospin doublet, the lower components of Dirac spinors look very similar, and the upper components of Dirac spinors satisfy the radial node relation $n(\kappa < 0) = n(\kappa > 0) + 1$. These indicate there is pseudospin symmetry. Compared with bound states, the pseudospin symmetry in resonant states is relatively worse. For every spin doublet, the upper components of Dirac spinors are similar, and the lower components of Dirac spinors satisfy the radial node relation $n(\kappa > 0) = n(\kappa < 0) + 1$. These mean there is spin symmetry. In comparison with the resonant states, the spin symmetry in the bound states is better.

In conclusion, the available single particle resonant levels in Pb isotopes appear clear shell structure. Although the energy and width splittings between the pseudospin (spin) doublets are relatively large, the symmetries are reserved well in their wave functions. The quality of pseudospin (spin) symmetry is correlated with the quantum numbers of single-particle states, isospin, and position of the states lying in mean field. Good pseudospin and spin symmetries are expected in the neutron-rich nuclei and these doublets with lower orbital angular momentum and lying near the zero energy surface.

Acknowledgements

This work is supported by the National Natural Science Foundation of China under Grant No. 11935001, 11575002, 11975167, 11535004 and 11761161001; the National Key R&D Program of China (Contract No. 2018YFA0404403); the National Major State Basic Research and Development of China under Grant No. 2016YFE0129300, and the Key Research Foundation of Education Ministry of Anhui Province under Grant No. KJ2018A0028.

References

[1] J.N. Ginocchio, Phys. Rep. 414 (2005) 165–261.
[2] H. Liang, J. Meng, S.G. Zhou, Phys. Rep. 570 (2015) 1–84.
[3] A. Leviatan, J.N. Ginocchio, Phys. Lett. B 518 (2001) 214–220.
[4] S. Shen, H. Liang, J. Meng, P. Ring, S. Zhang, Phys. Lett. B 781 (2018) 227–231.
[5] O. Haxel, J.H.D. Jensen, H.E. Suess, Phys. Rev. 75 (1949) 1766.
[6] M.G. Mayer, Phys. Rev. 75 (1949) 1969.

[7] K.T. Hecht, A. Adler, Nucl. Phys. A 137 (1969) 129.
[8] A. Arima, M. Harvey, K. Shimizu, Phys. Lett. B 30 (1969) 517.
[9] G.F. Wei, S.H. Dong, Phys. Lett. B 686 (2010) 288–292.
[10] W. Nazarewicz, P.J. Twin, P. Fallon, J.D. Garrett, Phys. Rev. Lett. 64 (1990) 1654.
[11] J.Y. Zeng, J. Meng, C.S. Wu, E.G. Zhao, Z. Xing, X.Q. Chen, Phys. Rev. C 44 (1991) R1745.
[12] Q. Xu, S.J. Zhu, J.H. Hamilton, A.V. Ramayya, J.K. Hwang, B. Qi, J. Meng, J. Peng, Y.X. Luo, J.O. Rasmussen, I.Y. Lee, S.H. Liu, K. Li, J.G. Wang, H.B. Ding, L. Gu, E.Y. Yeoh, W.C. Ma, Phys. Rev. C 78 (2008) 064301.
[13] W. Hua, X.H. Zhou, Y.H. Zhang, Y. Zheng, M.L. Liu, F. Ma, S. Guo, L. Ma, S.T. Wang, N.T. Zhang, Y.D. Fang, X.G. Lei, Y.X. Guo, M. Oshima, Y. Toh, M. Koizumi, Y. Hatsukawa, B. Qi, S.Q. Zhang, J. Meng, M. Sugawara, Phys. Rev. C 80 (2009) 034303.
[14] C. Delafosse, D. Verney, P. Marević, A. Gottardo, C. Michelagnoli, A. Lemasson, A. Goasduff, J. Ljungvall, E. Clément, A. Korichi, G. De Angelis, C. Andreoiu, M. Babo, A. Boso, F. Didierjean, J. Dudouet, S. Franchoo, A. Gadea, G. Georgiev, F. Ibrahim, B. Jacquot, T. Konstantinopoulos, S.M. Lenzi, G. Maquart, I. Matea, D. Mengoni, D.R. Napoli, T. Nikšić, L. Olivier, R.M. Pérez-Vidal, C. Portail, F. Recchia, N. Redon, M. Siciliano, I. Stefan, O. Stezowski, D. Vretenar, M. Zielinska, D. Barrientos, G. Benzoni, B. Birkenbach, A.J. Boston, H.C. Boston, B. Cederwall, L. Charles, M. Ciemala, J. Collado, D.M. Cullen, P. Désesquelles, G. de France, C. Domingo-Pardo, J. Eberth, V. González, L.J. Harkness-Brennan, H. Hess, D.S. Judson, A. Jungclaus, W. Korten, A. Lefevre, F. Legruel, R. Menegazzo, B. Million, J. Nyberg, B. Quintana, D. Ralet, P. Reiter, F. Saillant, E. Sanchis, Ch. Theisen, J.J. Valiente Dobon, Phys. Rev. Lett. 121 (2018) 192502.
[15] J.N. Ginocchio, Phys. Rev. Lett. 78 (1997) 436.
[16] J. Meng, K. Sugawara-Tanabe, S. Yamaji, P. Ring, A. Arima, Phys. Rev. C 58 (1998) R628–R631.
[17] J.N. Ginocchio, A. Leviatan, Phys. Lett. B 425 (1998) 1.
[18] J.S. Bell, H. Ruegg, Nucl. Phys. B 98 (1975) 151.
[19] J.N. Ginocchio, Phys. Rev. Lett. 95 (2005) 252501.
[20] A.S. de Castro, P. Alberto, R. Lisboa, M. Malheiro, Phys. Rev. C 73 (2006) 054309.
[21] L.B. Castro, Phys. Rev. C 86 (2012) 052201.
[22] A. Leviatan, Phys. Rev. Lett. 92 (2004) 202501.
[23] A. Leviatan, Phys. Rev. Lett. 103 (2009) 042502.
[24] H. Liang, P. Zhao, Y. Zhang, J. Meng, N.V. Giai, Phys. Rev. C 83 (2011) 041301(R).
[25] J.N. Ginocchio, J. Phys. Conf. Ser. 267 (2011) 012037.
[26] J.Y. Guo, Phys. Rev. C 85 (2012) 021302.
[27] J.Y. Guo, S.W. Chen, Z.M. Niu, D.P. Li, Q. Liu, Phys. Rev. Lett. 112 (2014) 062502.
[28] S.W. Chen, J.Y. Guo, Phys. Rev. C 85 (2012) 054312.
[29] D.P. Li, S.W. Chen, J.Y. Guo, Phys. Rev. C 87 (2013) 044311.
[30] D.P. Li, S.W. Chen, Z.M. Niu, Q. Liu, J.Y. Guo, Phys. Rev. C 91 (2015) 024311.
[31] H. Liang, S. Shen, P.W. Zhao, J. Meng, Phys. Rev. C 87 (2013) 014334.
[32] S. Shen, H. Liang, P. Zhao, S. Zhang, J. Meng, Phys. Rev. C 88 (2013) 024311.
[33] Q. Xu, Eur. Phys. J. A 51 (2015) 1.
[34] T.T. Sun, W.L. Lu, S.S. Zhang, Phys. Rev. C 96 (2017) 044312.
[35] R. Lisboa, P. Alberto, B.V. Carlson, M. Malheiro, Phys. Rev. C 96 (2017) 054306.
[36] Y.X. Guo, H. Liang, Phys. Rev. C 99 (2019) 054324.
[37] J. Meng, K. Sugawara-Tanabe, S. Yamaji, A. Arima, Phys. Rev. C 59 (1999) 154–163.
[38] O. Sorlin, M.-G. Porquet, Prog. Part. Nucl. Phys. 61 (2008) 602.
[39] W.H. Long, T. Nakatsukasa, H. Sagawa, J. Meng, H. Nakada, Y. Zhang, Phys. Lett. B 680 (2009) 428.
[40] I. Hamamoto, Phys. Rev. C 85 (2012) 064329.
[41] G.M. Hale, R.E. Brown, N. Jarmie, Phys. Rev. Lett. 59 (1987) 763.
[42] J.R. Taylor, Scattering Theory: The Quantum Theory on Nonrelativistic Collisions, John Wiley Sons, New York, 1972.
[43] B.N. Lu, E.G. Zhao, S.G. Zhou, Phys. Rev. Lett. 109 (2012) 072501.
[44] B.N. Lu, E.G. Zhao, S.G. Zhou, Phys. Rev. C 88 (2013) 024323.
[45] V.I. Kukulin, V.M. Krasnopl'sky, J. Horácek, Theory of Resonances: Principles and Applications, Kluwer, Dordrecht, 1989.
[46] S.C. Yang, J. Meng, S.G. Zhou, Chin. Phys. Lett. 18 (2001) 196.
[47] S.S. Zhang, J. Meng, S.G. Zhou, G.C. Hillhouse, Phys. Rev. C 70 (2004) 034308.
[48] S.S. Zhang, M.S. Smith, Z.S. Kang, J. Zhao, Phys. Lett. B 730 (2014) 30–35.
[49] E.N. Economou, Green's Function in Quantum Physics, Springer-Verlag, Berlin, 2006.
[50] T.T. Sun, W.L. Lu, L. Qian, Y.X. Li, Phys. Rev. C 99 (2019) 034310.
[51] J. Aguilar, J.M. Combes, Commun. Math. Phys. 22 (1971) 269;
E. Balslev, J.M. Combes, Commun. Math. Phys. 22 (1971) 280.
[52] B. Simon, Commun. Math. Phys. 27 (1972) 1.
[53] J.Y. Guo, X.Z. Fang, P. Jiao, J. Wang, B.M. Yao, Phys. Rev. C 82 (2010) 034318.
[54] A.T. Kruppa, Phys. Lett. B 431 (1998) 237.
[55] R. Suzuki, T. Myo, K. Katō, Prog. Theor. Phys. 113 (2005) 1273.
[56] M. Shi, J.Y. Guo, Q. Liu, Z.M. Niu, T.H. Heng, Phys. Rev. C 92 (2015) 054313.
[57] X.X. Shi, M. Shi, Z.M. Niu, T.H. Heng, J.Y. Guo, Phys. Rev. C 94 (2016) 024302.
[58] M. Shi, X.X. Shi, Z.M. Niu, T.T. Sun, J.Y. Guo, Eur. Phys. J. A 53 (2017) 40.
[59] N. Li, M. Shi, J.Y. Guo, Z.M. Niu, H. Liang, Phys. Rev. Lett. 117 (2016) 062502.
[60] Z. Fang, M. Shi, J.Y. Guo, Z.M. Niu, H.Z. Liang, S.S. Zhang, Phys. Rev. C 95 (2017) 024311.
[61] P. Ring, Prog. Part. Nucl. Phys. 37 (1996) 193.
[62] D. Vretenar, A.V. Afanasjev, G.A. Lalazissis, P. Ring, Phys. Rep. 409 (2005) 101.
[63] J. Meng, H. Toki, S.G. Zhou, S.Q. Zhang, W.H. Long, L.-S. Geng, Prog. Part. Nucl. Phys. 57 (2006) 470.
[64] J.Y. Guo, R.D. Wang, X.Z. Fang, Phys. Rev. C 72 (2005) 054319.
[65] S.S. Zhang, B.H. Sun, S.G. Zhou, Chin. Phys. Lett. 24 (2007) 1199.